Biomedical Signal Processing and Control 6 (2011) 85–93

Contents lists available at ScienceDirect

Biomedical Signal Processing and Control

journal homepage: www.elsevier.com/locate/bspc

Examination of time-varying kinematic responses to support surface disturbances

S. Gurses[a,*], R.V. Kenyon[b], E.A. Keshner[c,d]

[a] Middle East Technical University, Dept. of Engineering Sciences, Ankara 06531, Turkey
[b] University of Illinois at Chicago, Dept. of Computer Science, Chicago, IL 60607, USA
[c] Dept. of Physical Therapy, Temple University, Philadelphia, PA 19095, USA
[d] Dept. of Electrical and Computer Engineering, Temple University, Philadelphia, PA 19095, USA

ARTICLE INFO

Article history:
Received 8 December 2009
Received in revised form 5 April 2010
Accepted 1 June 2010
Available online 8 July 2010

Keywords:
Posture
Statistical model
Postural strategy
Spectral content
Time dependency

ABSTRACT

To examine the evolution of inter-segmental coordination over-time, a previously developed multivariate model of postural coordination during quiet stance by Kuo et al. [1,2] has been extended. In the original model, postural coordination was treated as an eigenvalue–eigenvector problem between two segmental degrees of freedom represented by angular displacements of the trunk and shank. Strategies of postural coordination were then identified using the sign of the covariance between the two segments' angular displacements. In contrast to the original model, the current model first subdivided the entire trial into smaller time segments, comprising four cycles of perturbation, i.e., a 16 s window. This window marched along the data advancing in 8.3 ms steps, each time performing the computation from the original model on the terms of the covariance matrix. The resulting time-segment-dependent postural strategies estimated the changes in posture control that took place over the course of the experiment. In addition to the statistical modeling, the auto-power spectrums and cross-spectral density function estimates for the entire trial, as well as for the individual time segments, were analyzed. In these experiments subjects experienced a 0.25 Hz sinusoidal perturbation of a platform while exposed to a virtual reality environment. The data we collected showed that the statistical and spectral characteristics across the entire trial may differ from individual time segments of the same trial indicating time-varying postural behavior. Comparison of these results from young and elderly subjects revealed that the time dependency observed in postural behavior was sensitive to aging. The young population managed to be consistent in their postural behavior throughout the entire trial and responded to the perturbation frequency with an out-of-phase response between the postural segments. Elderly subjects, however, demonstrated inconsistent postural behaviors as they switched back and forth between different postural coordination patterns within a trial.

1. Introduction

Previous studies have shown that sway during quiet stance [2–8] exhibits non-linear and time-varying behavior suggesting shifting mechanisms for control. Furthermore, Creath et al. [7] have proposed that the whole body behaves like a multi-link pendulum during quiet stance and has two simultaneously co-existing excitable modes. Each mode exhibits a separate eigen-frequency containing characteristic phase relationships that are functions of the frequency at which the individual segments oscillate. Time-varying spectral characteristics in head and trunk stabilization to an external perturbation have also recently been reported [9], implying that segmental adaptation to an external disturbance may continuously shift between several control mechanisms. Kuo et al. [1] developed a multivariate model of postural coordination during quiet stance. In their model, postural coordination was treated as an eigenvalue–eigenvector problem between two segmental degrees of freedom represented by angular displacements of the trunk and lower limb. A multivariate description of postural sway was constructed to reveal two independent kinematic (spatial) relationships (hip and ankle eigen-movements) each defining a postural strategy [1]. A hip or ankle strategy of postural coordination was identified using the sign of the covariance between angular displacements of the two segments.

To understand the non-linear and time-varying properties involved in posture control we extended the Kuo et al. model [1] by dividing a trial into several time segments and then analyzing these time segments to identify whether a hip or ankle strategy predominated. The ensuing data provided us with a pic-

* Corresponding author. Tel.: +90 312 210 4461; fax: +90 312 210 4462.
E-mail addresses: senih@metu.edu.tr (S. Gurses), kenyon@uic.edu (R.V. Kenyon), ekeshner@temple.edu (E.A. Keshner).

1746-8094/$ – see front matter © 2010 Elsevier Ltd. All rights reserved.
doi:10.1016/j.bspc.2010.06.002

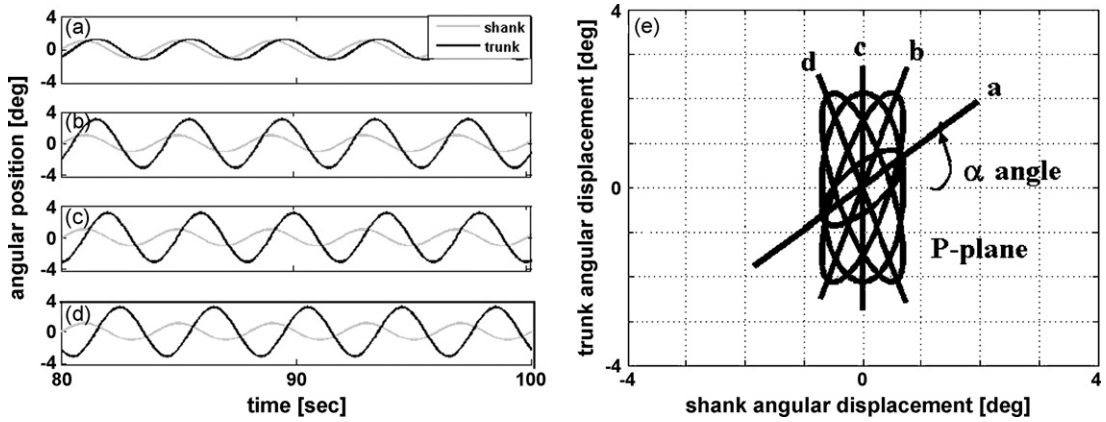

Fig. 1. (a) A 20 s portion of a 140 s time series simulation of trunk and shank angular position data during a 0.25 Hz platform translation. (a and b) Amplitude of the trunk's motion decreased by a factor of 3 with respect to the angular motion of the shank but the phase angle in between remained constant ($\varphi = \pi/4$); (c and d) amplitude of the trunk's angular motion with respect to the angular motion of the shank remained constant but φ shifted ($\pi/2$ and $3\pi/4$, respectively); (e) elliptical representation of the data simulated in a–d on the *P*-plane.

ture of the evolution of inter-segmental coordination across a trial. Our results from examining both young and elderly populations showed that a majority of the young subjects exhibited a consistent postural control strategy across time, whereas the elderly subjects were more likely to change their postural control strategy from one time segment to the next. Moreover, the characteristics of the spectral components were found to be stable across time in the young subjects, pointing to a consistent postural strategy, that is, an out-of-phase relationship at the perturbation frequency. As observed by Kuo [2], elderly subjects demonstrated large variability in their postural responses. Our model extended his findings by revealing that many frequencies were involved in their postural coordination.

2. Methods

2.1. Previous model

The eigen-structure of human postural sway has been explored through a statistical model. Kuo et al. [1,2] used a multivariate description of postural sway to reveal two independent kinematic (spatial) relationships (eigen-movements) each defined as a postural strategy: an inverted pendulum (ankle strategy) or a bending at the hip (hip strategy) [10]. In this model, the output vector θ for the kinematic relationship between two segments was defined by Eq. (1), where θ_a and θ_h represent the angle between the foot and the shank (ankle) and the angle between the leg and the trunk (hip), respectively. Variability between the motions of these two segments was calculated using the covariance matrix Q (Eq. (2)) where n is the number of data points. Matrix Q is a symmetric matrix, where covariance of ankle and hip (σ_{ah}) is equal to the covariance of hip and ankle (σ_{ha}). Further, σ_a^2 and σ_h^2 in (Eq. (2)) are variance of angular motion at ankle and hip, respectively. Eigenvalues and related eigenvectors of this covariance matrix were computed to extract the spatial relation between the angular displacement of the trunk and the shank. Eigenvector 1 was defined as representing an "inverted pendulum" strategy, where both segments rotate in the same direction. Similarly, eigenvector 2 was defined as representing the "hip strategy" where the two segments rotate in opposite directions. The amplitudes of the related segmental motions defined the associated eigenvalue of the eigenvectors since this scaled the length of the vectors and did not affect their direction (Fig. 1e).

$$\theta[\,\theta_a \quad \theta_h\,] \tag{1}$$

$$Q = \frac{1}{n-1}\sum_{i=1}^{n}(\theta_i - \bar{\theta})^T(\theta_i - \bar{\theta}) = \begin{bmatrix} \sigma_a^2 & \sigma_{ah} \\ \sigma_{ha} & \sigma_h^2 \end{bmatrix} \tag{2}$$

Geometric representation of the solution: Kuo et al. [1] used a two degree of freedom (DOF) statistical multivariate model to analyze postural sway. Plotting the angular motion of the shank versus the trunk resulted in an ellipse which lay in a plane labelled *P* (Fig. 1). The ellipse graphically demonstrated the dominant postural strategy used by the subject throughout the selected interval of time. The major and minor axes of the ellipse in the plane *P* represented two spatial relationships (eigenvectors) between the angular motion of the shank and the trunk. The covariance matrix *Q* was decomposed (diagonalization) to identify these spatial relationships inherent in the ellipse. The angle of the ellipse's major axis (α) designated the eigenvector associated with the largest eigenvalue of the covariance matrix, *Q*. A counterclockwise rotation of the angle α (from the + x-axis) was defined as positive. The dominant postural strategy used by the subject was deemed an ankle strategy if $\pi/2 < \alpha < 0$ (quadrant I response), or a hip strategy if $\pi < \alpha < \pi/2$ (quadrant II response).

2.2. Time domain statistical model

Kuo et al. [1,2] used the subject's entire time–response during a trial to characterize their postural behavior. In this study, however, we investigated how postural characteristics varied during the period of a trial by subdividing each trial into time segments. By analyzing each time segment individually we could examine the variability of the postural coordination exhibited by the subject during the trial. Consequently, the terms of the covariance matrix *Q* (in Eq. (2)) became a function of the *m* time segments that comprised the experimental data. That is, the covariance term σ_{ah} (in Eq. (2)) is applied to a single time segment where *T* covers the time interval for a single time segment as seen in Eq. (3).

$$\sigma_{ah} = \frac{1}{T}\int_0^T \{\theta_a(t) - \bar{\theta}_a\}\{\theta_h(t) - \bar{\theta}_h\}dt \tag{3}$$

In essence, (3) characterizes the postural behavior for a specific time segment. When this analysis is performed for each time segment that is part of the entire trial, σ_{ah} becomes a function of time.

Since only the sign of the covariance can indicate a change in the postural strategy, the covariance was normalized with respect

to the magnitude of the motion of each of the body segments. This normalization transformed the covariance into the correlation coefficient thereby making its sign the prevalent variable (Eqs. (4) and (5)) [11]. As a result, the sign of the covariance of the motion between shank and trunk was used to extract the dominant eigenvector associated with the largest eigenvalue.

$$\rho_{ah} = \frac{\sigma_{ah}}{\sqrt{\sigma_{aa} \cdot \sigma_{hh}}} \tag{4}$$

where,

$$-1 \leq \rho_{ah} \leq 1 \tag{5}$$

2.3. Frequency domain analysis

In addition to the statistical analysis above, power spectral density (PSD) function estimates and cross-spectral density (CSD) function estimates of shank and trunk motion for both the entire period of trial and for the individual time segments were also analyzed. The aggregate PSD and CSD for each time segment throughout the data will reveal any time-dependency effects that may exist in eigen-movements and related eigen-frequencies of the postural coordination. CSD estimates of the shank versus the trunk were then computed for each of the time segments to explore any time dependency that might be exhibited in the phase relationship between the shank and the trunk. Finally, the coherence function estimates between the shank and trunk motion were computed to examine how the motions of the two body segments were coupled at the driving frequency.

2.4. Experimental apparatus and the experimental protocol

Our model was applied to previously collected data from 7 healthy young (25–38 years) and 6 healthy elderly (60–78 years) subjects standing on a platform that translated in the anterior–posterior direction at 0.25 Hz for 180 s for the young and 90 s for the elderly. All subjects gave informed consent according to the guidelines of the Institutional Review Board of Feinberg School of Medicine, Northwestern University to participate in this study. All subjects had no history of central or peripheral neurological disorders or problems related to movements of the spinal column (e.g., significant arthritis or musculoskeletal abnormalities) and a minimum of 20/40 corrected vision.

Three-dimensional kinematic data from the body segments were collected at 120 Hz using a motion analysis system (Optotrak, Northern Digital Inc., Ontario, Canada) with a resolution of 0.1 mm. Infrared markers placed at C_7 and the greater trochanter were used to calculate trunk angular position relative to earth vertical. Shank angular position was defined as the angle between the lateral femoral condyle and the lateral malleolus relative to earth vertical. Sled motion was subtracted from the linear motion of each segment prior to calculating segmental motion. Motion of the shank was removed from motion of the trunk to reveal motion of the trunk with respect to the shank (θ_h). The shank was examined with respect to the platform (θ_a).

Subjects stood in front of a virtual environment that provided motion of the visual field. The virtual environment scene was driven by an external signal summed with movements of the subject's head transmitted from the motion analysis system [12]. The time series for the shank and trunk angular displacements were detrended linearly and bandpass filtered with a cut-off frequency of 0.05 and 50 Hz. The first and last 20 s of each trial were removed leaving 140 s of the 180 s trials and 70 s of the 90 s trials to be analyzed. A 16 s window that marched along the data advanced 8.3 ms per step (1/120) to explore the time variations for each data sample.

3. Results

3.1. Experimental data

Fig. 2 shows a representative example of the behavior exhibited by the majority (86%) of the young population and a minority of the elderly population (17%) when experiencing a 0.25 Hz platform perturbation with an earth-fixed scene. The single ellipse formed by using the entire response from this condition (Fig. 2a) and the multiple ellipses that resulted when these same data were subdivided into time segments (Fig. 2e) show similar characteristics. The pattern of postural behavior emerging from each method of analysis shows a well defined ellipse whose major axis lies in quadrant II of the P-plane [$R^2 = 0.78$]. The regularity of this response can be seen in Fig. 2d where σ_{ah}, the covariance term, is plotted as a function of time. It has been found that σ_{ah} has a consistent negative value throughout the epoch of the trial. The negative value of σ_{ah} confirms that the angle α, formed by the major axis of the ellipse, is in the second quadrant of the plane P for both the overall and the segmented ellipses (Fig. 2a and e). A minor axis of the ellipse also emerges from the diagonalization of the covariance matrix Q. Since this axis is orthogonal to the major axis, it is in the first quadrant for these same data.

To reveal the frequency components of the postural strategies used, we examined the power spectral density (PSD) of the two segmental motions over the entire trial and at each time segment. The PSD across the entire trial (Fig. 2b) shows that almost all of the power in this response occurs at the perturbation frequency (0.25 Hz). The PSD as a function of the individual time segments (Fig. 2f) shows approximately the same characteristic as does the entire trial analysis. However, the peak power varies somewhat over the course of the trial as seen in the middle of the time segment data. The CSD for the entire trial (Fig. 2c) reveals that these two body segments have a predominant out-of-phase (180°) (Φ: phase angle; $-\pi < \Phi < -\pi/2$ or $\pi/2 < \Phi < \pi$) relationship at the perturbation frequency. When the trial was analyzed as a function of time (Fig. 2g), we found little difference in the phase at the disturbance frequency when compared to that of the entire trial. Furthermore, we find that the motion of the trunk was larger than that of the shank. The two body segments are coupled and their motion is coherent with the perturbation at the 0.25 Hz frequency as shown in the coherence function between motion of the two segments (Fig. 2h). The power for the in-phase relation of the two body segments (minor axis of the ellipse or ankle strategy) is small in the PSDs.

In contrast, a majority (83%) of the elderly subjects and a minority of the young subjects (14%) exhibited an overall ellipse that was not representative of the ellipses that emerged as a function of time. The single ellipse fitted by using the entire trial of a representative elderly subject (Fig. 3a) falls in the second quadrant with an R^2 of 0.43. When these data were examined as a function of time, the individual ellipses that emerged changed in orientation, size, and shape (Fig. 3e). Thus, according to these data, unlike the majority of young subjects, a majority of the elderly do not exhibit a consistent sign for the covariance term (Fig. 3d). The value of $\sigma_{ah}(t)$ varied between ± 1 across the time of the trial. These data quantify the extent to which α shifted between quadrants I and II.

Examining the ensemble PSD produced for the shank and trunk using data from the entire epoch of the trial, we found that the power at the trunk was greater than that at the shank for all frequencies (Fig. 3b). Also, the frequency at which the main peak occurred (trunk: 0.13 Hz; shank: 0.2 Hz) was different from the driving frequency (0.25 Hz). Finally, additional power can be seen up to 0.75 Hz for the trunk and 0.5 Hz for the shank.

From the ensemble CSD phase (Fig. 3c), we found an out-of-phase relationship between the trunk and shank at all frequencies. The time-segmented PSDs (Fig. 3f) showed a more complex fre-

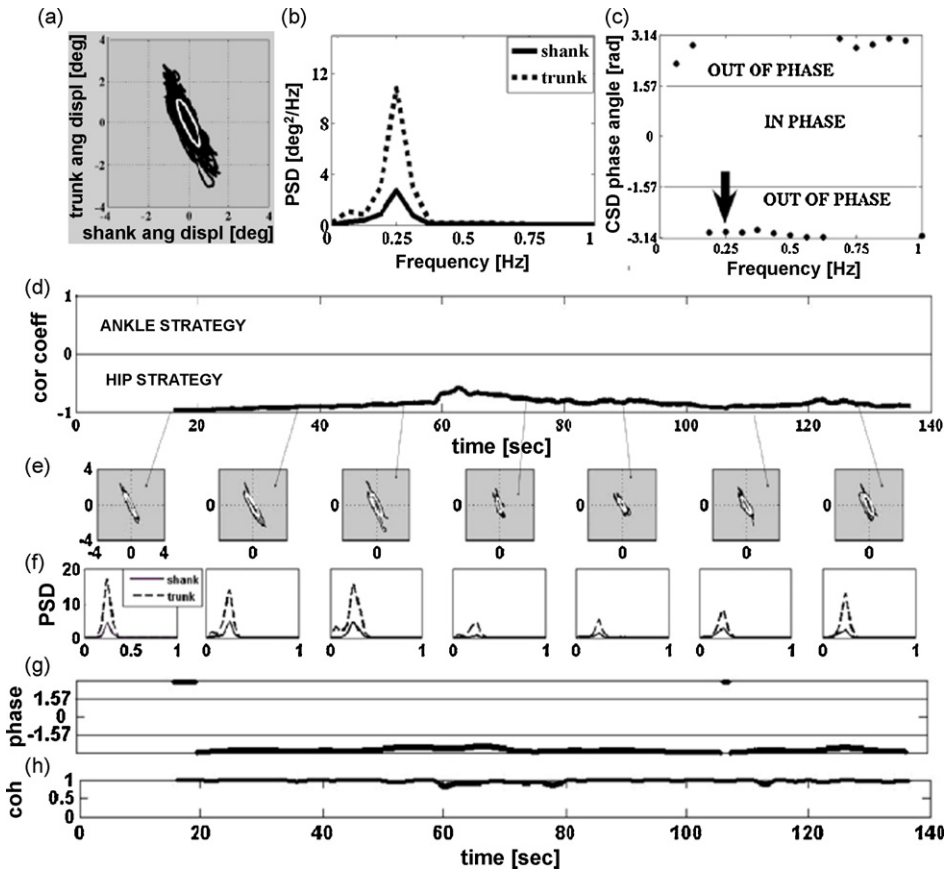

Fig. 2. (a) Plot of an ellipse fit (white) to the 140-s response (black) of angular position of the shank with respect to platform (x-axis) plotted against angular position of the trunk with respect to shank (y-axis) from a typical young subject. All subsequent analyses used these data. (b) PSD estimates of the shank (solid line) and trunk (dashed line) across the entire trial. (c) CSD estimates for the entire trial (only phase angle is shown). Arrow indicates 0.25 Hz. (d) Correlation coefficient, $\rho_{ah}(t)$, between shank and trunk, where t stands for time. (e) Ellipses fit to the shank versus trunk response for seven different time segments. Arrows show the corresponding time segments. (f) PSD at each time segment: shank (solid) and trunk (dashed). (g) CSD at each time segment, (φ at 0.25 Hz). (h) The coherence function estimate at each time segment.

quency relationship with time. The postural responses exhibited peak power at multiple frequencies instead of a single peak at the perturbation frequency. In addition, the dominant power shifted back and forth between shank and trunk as a function of time. Furthermore, the phase at the disturbance frequency (0.25 Hz) shifted from in-phase to out-of-phase as a function of time (Fig. 3g). In 10% of the time segments presented in Fig. 3, the peak power was at the shank and the motion was in-phase (Fig. 3g); for the remaining 90%, peak power was at the trunk and the motion was generally out-of-phase. Accordingly, motion between the trunk and shank or between the body and the platform was rarely coherent (Fig. 3h).

3.2. Simulation of the experimental data

Data from our subjects indicated that postural responses could be grouped into two general categories: responses dominated by a single frequency [Case 1] or responses that contained significant power at many frequencies [Case 2].

3.2.1. Case 1

For Case 1 we used a single sinusoid at 0.25 Hz to simulate each postural segment's motion (albeit noiseless); i.e., motion of the trunk with respect to the shank (θ_h) and motion of the shank with respect to the platform (θ_a). We first varied the amplitude of simulated trunk motion relative to the amplitude of shank motion by a factor of 1–3 (Fig. 1a and b, respectively), while the phase relationship between the two segments was held constant over the interval of the simulation ($\varphi = \pi/4$). We then changed the phase angle, φ between the shank and the trunk from $\pi/4$ to $2\pi/4$, and $3\pi/4$ (Fig. 1c and d, respectively), while the amplitude of the trunk's angular motion with respect to the angular motion of the shank remained constant. According to these conditions, Eq. (1), was now defined as:

$$\theta(A, t, \varphi) = [A_a \sin(\omega t + \varphi) A_h \sin(\omega t)] \tag{6}$$

where A_a and A_h were the magnitudes of the shank and the trunk segmental motion, respectively, ω was the driving frequency of the system (fixed at 0.25 Hz), t represented time and φ was the phase angle between the two segments' angular motion. Covariance σ_{ah} between ankle and hip's motion (Eq. (3), the cross-talk term in covariance matrix Q in Eq. (2)) was then calculated where T was the total recording time for n cycles of perturbation; i.e., $T = 2\pi n/\omega$:

$$\sigma_{ah}(A, \varphi) = \frac{1}{T} \int_0^T A_a \sin(\omega t + \varphi) \cdot A_h \sin(\omega t) \mathrm{d}t \tag{7}$$

The solution for Eq. (7) was:

$$\sigma_{ah}(A, \varphi) = \frac{A_a A_h \cos(\varphi)}{2} \tag{8}$$

3.2.2. Case 2

Our data and that of others' [5,6,9,13,14] have shown that the response to a disturbance with even a single frequency can result in a response that contains significant power at many frequencies. As a first step at understanding this complex response, we simulated responses using two frequencies, which is the simplest case that

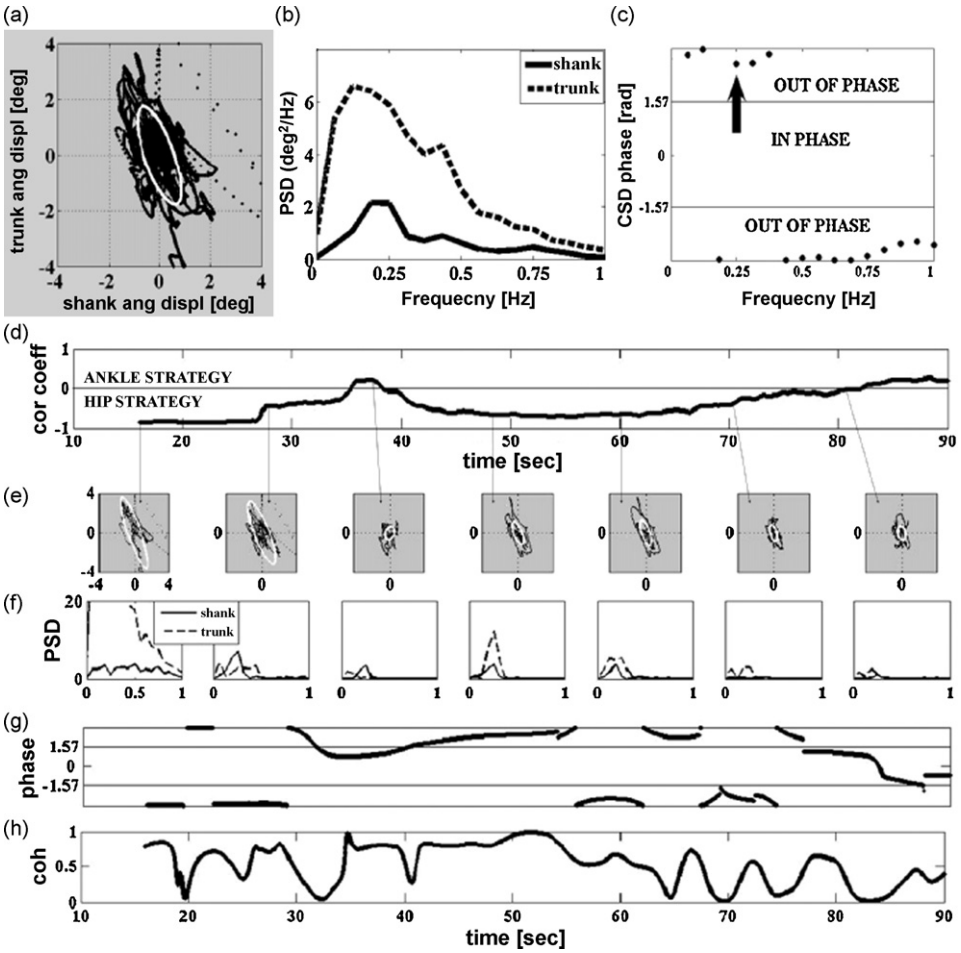

Fig. 3. (a) Plot of an ellipse fit (white) to the 90-s response (black) of angular position of the shank with respect to platform (x-axis) plotted against angular position of the trunk with respect to shank (y-axis) from a typical elderly subject. Data in b–h are structured identical to Fig. 2.

can be defined for a multi-frequency response. For this condition, Eq. (1), was re-defined as:

$$\theta(A, \omega, \varphi, t)\left[\sum_{i=1}^{n} A_i^a \sin(\omega_i t + \varphi_i) \quad \sum_{i=1}^{n} A_i^h \sin(\omega_i t)\right] \tag{9}$$

where A_i^a and A_i^h were the magnitudes of the shank and trunk segmental motion, respectively for the ith sinusoidal involved in the response with the phase φ_i between the ankle and hip's angular motion, while t represented time. It is important to note that some of the sinusoids involved in the response might be representing the ith mode of the postural dynamics with the related eigen-frequency ω_i. The phase relationship between the ankle and hip, φ_i, was once again held constant throughout an individual simulation. In contrast to Case 1, using Eq. (9) instead of Eq. (6) also made θ a function of the frequencies ω_i involved in the response.

Covariance, σ_{ah}, between ankle and hip motion was then calculated through Eq. (10):

$$\sigma_{ah} = \frac{1}{T}\int_0^T \sum_{i=1}^{n} A_i^a \sin(\omega_i t + \varphi_i) \cdot \sum_{i=1}^{n} A_i^h \sin(\omega_i t) \cdot dt \tag{10}$$

Given that the simulated response involved harmonics; i.e., integer multiples of the fundamental (perturbation) frequency, the solution for Eq. (10) became ($n = 2$): (see Appendix A)

$$\sigma_{ah}(A_i, \varphi_i) = \frac{A_1^a A_1^h}{2}\cos(\varphi_1) + \frac{A_2^a A_2^h}{2}\cos(\varphi_2) \tag{11}$$

Examining the covariance, σ_{ah} (Eq. (11)), as a function of A_i, and φ_i, we realized that the *sign* of the covariance depended at least on both the magnitude and phase of the ankle and hip angular motion. This was in contrast to the first case, where the *sign* of the covariance term, σ_{ah}, depended only on the phase between the angular motion of the ankle and hip (see Eq. (8)).

For Case 2, we used two frequencies, 0.25 and 0.57 Hz, which were within the range of the response power measured in our data [although these frequencies could be arbitrarily chosen within the response range of the subject]. Furthermore, the phase relationship between the ankle and hip was constant at each frequency: the angular motion of the ankle and hip was in-phase at the lower frequency while at the higher frequency it was out-of-phase (Fig. 4c). We then applied two different spectrums of power for these two frequencies. In both of the spectrums, the following scheme was employed: the power of the ankle response was greater than power of the hip response at 0.25 Hz but at 0.57 Hz, the power of the hip response was higher than the power of the ankle response (Fig. 4b and e). However, the peak in the spectral response [or dominant power of the response] took place at 0.25 Hz in the first spectral pattern (Fig. 4b), while the dominant power of the response was at 0.57 Hz in the second spectral pattern (Fig. 4e).

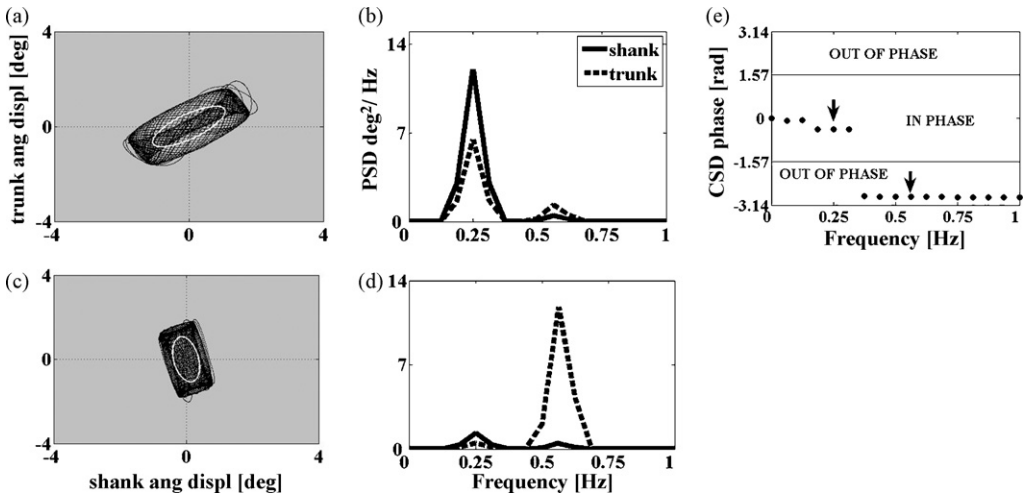

Fig. 4. The first spectral pattern (a and b): 140-s simulated response of the angular position of the shank versus the angular position of the trunk with the elliptical representation of the data on the plane *P*, (a). The major axis of the ellipse lies in quadrant I. The power seen at 0.25 Hz (perturbation frequency) in the simulated response of the subject is greater than the power seen at 0.57 Hz (b). The second spectral pattern (c and d): 140-s simulated response of the angular position of the shank versus the angular position of the trunk with the elliptical representation of the data on the plane *P* with the major axis of the ellipse lying in the quadrant II (c). The power seen at 0.57 Hz in the simulated response of the subject is greater than the power seen at the perturbation frequency (0.25 Hz) in the response of the subject (d). The phase relationship between the shank and trunk's angular motion were held constant at each frequency (e). The arrows at e show the phase angles at the two frequencies involved in the simulated response of the subject.

The simulations for both Case 1 and Case 2 help clarify how their respective equations represent our data. For Case 1, the behaviors shown in Fig. 3 display two important features of the integral given in Eq. (7): that both amplitude and phase of the segmental motion can be changed across time. Our simulations also confirm the conclusions derived from Eq. (8), that the only way to shift the ellipses from one quadrant to the other was to change the value of φ. Thus, changing only the amplitude of segmental motion does not produce a switch from one quadrant to another. When $0 < \varphi < \pi/2$, covariance between ankle and hip remained positive, i.e., the segments co-varied in a positive direction regardless of their amplitudes (Fig. 1a and b). Similarly, when $\pi/2 < \varphi < \pi$, covariance between ankle and hip remained negative, i.e., the segments co-varied in a negative direction (Fig. 1d). If $\varphi = \pi/2$, the result of the integral was zero and the response aligned with the axes of plane *P* (Fig. 1c). However, when the value of φ was set to $\pi/4$, $\pi/2$ and $3\pi/4$ (Eqs. (6)–(8)), the ellipses shifted between quadrants regardless of amplitude (Fig. 1e).

However, our simulations from Case 2 show that there is more than one way to shift the ellipses from one quadrant to the other when there are two frequencies in the response, where the modes of segmental motion have opposite phase relationships. In contrast to Case 1, the covariance term σ_{ah} can change sign either with a change in the amplitude of motion in any of the postural segments (Eq. (11)) or with a change in the ratio of the frequencies ($k = \omega_1/\omega_2$) emerging in the subject's response (see Appendix A). For Case 2, the resulting behaviors shown in Fig. 4a and d display one of three (see Appendix A) important features of the integral given in Eq. (10): that a change in the amplitude of the postural segments' motion in time causes a shift in the postural behavior. Thus, in the case of a multi-frequency response where there can be an in or out-of-phase relationship dependent on frequency, changing only the amplitude of segmental motion could produce a switch from one quadrant to another when the phase at each frequency remained constant. For example, a quadrant I ankle strategy response (Fig. 4a) exhibits its dominant power at the perturbation frequency (Fig. 4b) with an in-phase relationship between ankle and hip (Fig. 4c). Alternatively, a quadrant II hip strategy response (Fig. 4d) can be achieved by shifting power to the other frequency in the spectrum of the response (Fig. 4e) without changing the phase relationships between the ankle and hip motion. Finally, if the power spectrum remains constant, a flip in the phase would produce the same result (not shown). Protocols and results obtained from the experiments and the simulations are summarized in Table 1.

Table 1
Summary of the protocols and obtained results from the experiments and the simulations.

Stimulus: sinusoidal A-P platform motion		
Experiments		
Population	Strategy [quadrant]	Consistency
86% of young and 17% of elderly	Lumped responses: hip [QII] Responses over-time: hip [QII]	Only QII Frequency response is at the perturbation frequency only
14% of young and 83% of elderly	Lumped responses: hip [QII] Responses over-time: ankle [QI] and hip [QII]	Variable between QI and QII Frequency response is at many frequencies
Stimulus: sinusoidal A–P platform motion		
Simulations	Conditions	Result
Case 1	Single dominant frequency; phase constant	only phase between hip and ankle can cause a change in quadrants.
Case 2	Multiple dominant frequencies [2 freq]; phase constant	either amplitude or phase [or both] can cause a change in quadrants.

4. Discussion

Our analysis shows that the majority of the young adult subjects used a "hip strategy" when compensating for our postural disturbance. The use of the "hip strategy" at a single frequency meant that they only needed to control the phase of the segmental response to maintain a uniform postural coordination. Variability in the postural kinematics of an otherwise homogenous cohort (healthy young adults) has been noted previously when the sen-

sory array has been significantly altered [2,15] or when subjects were asked to perform a concurrent cognitive task [16–18]. But when neither sensory alterations nor additional attention demands were present, healthy young subjects exhibited consistent ground reaction forces and lower limb EMG responses after the first few seconds of a 30 s trial of tandem stance [19]. However, given the same single frequency stimulus perturbation, elderly adults exhibited multiple dominant frequencies in their response. The appearance of multiple frequencies required that they control phase, magnitude, and the frequency of the response to organize an effective postural strategy. In fact, elderly subjects were observed to switch their response strategies between hip and ankle through a continuum of these synergies throughout the period of the trial [20,21].

During quiet stance, Creath et al. [7] identified postural behaviors that had co-existing excitable modes, each with separate eigen-frequencies in young adults. Our analysis indicates that when a single dominant input perturbs the system, a more consistent strategy is organized by the young adults to counteract the disturbance with almost the entire power of the response observed at the perturbation frequency. Thus, postural control in young adults can demonstrate linear system behavior. On the contrary, our results indicate that the elderly subjects are unable to harness their control mechanisms to match the most relevant frequency for the postural disturbance. Rather, the power of the elderly subjects' response is scattered over a broad, nearly featureless spectrum. This spectrum resembles a chaotic regime developed by transitions originating from non-linearities in the postural dynamics which have started from a few independent oscillations at well defined frequencies [22]. In fact, responses observed over long periods of postural disturbance would suggest that higher order processes (i.e., attention and perception) are supplying the non-linear dynamics to the postural behaviors recorded in these experiments [23–28]. The subsequent demands of controlling multiple response parameters will increase the complexity of the postural solution and may ultimately require that greater attention be given to the organization of the response. Diminished capacity to attend to more than one task during postural demands has been cited as a causative factor for instability in the elderly [29]. Thus, these findings have significant implications for the control of posture in the elderly, particularly when placed in environments that contain more than one input that may have an impact on our ability to maintain an upright posture [30,31].

Any possible existence of chaotic behavior or motion, and the potential physiological mechanisms responsible for the behavioral difference observed between young and elderly subjects, deserves to be analyzed. We have demonstrated that a time domain statistical model provides a more sensitive measure of postural organization than the more commonly used measure of center of pressure [19,32–35] which is a global outcome measure and does not fully describe segmental postural behaviors. A perturbed postural system does not necessarily respond only at the driving frequency [6,7,13] and one of the advantages of this statistical model is that it is not limited to describing behavior just at the driving frequency. We believe that this model will enable us to explore the full bandwidth of adaptive postural control during complex tasks.

Acknowledgements

This work was supported by National Institute of Health grants DC01125 and DC05235 from the NIDCD and AG16359 from the NIA. We gratefully acknowledge VRCO for supplying CAVE library software and the Ascension Tracker Daemon.

Appendix A.

If the response of the subject to the perturbation involves only one frequency then the covariance between the angular motions of the shank (θ_a) and the trunk (θ_h) can be written as (Eq. (7) rewritten):

$$\sigma_{ah}(A,\varphi) = \frac{1}{T}\int_0^T A_a \sin(\omega t+\varphi)\cdot A_h \sin(\omega t)dt \tag{A1}$$

where $T = n2\pi/\omega$ and ω is the driving frequency. n is an integer showing the number of cycles of perturbation. If we define $\theta = \omega t$ and change the variable of the integral in Eq. (A1) from time t to angle θ:

$$\sigma_{ah}(A,\varphi) = \frac{1}{n2\pi}\int_0^{n2\pi} A_a \sin(\theta+\varphi)\cdot A_h \sin(\theta)\cdot d\theta \tag{A2}$$

The solution of the integral in Eq. (A2) is:

$$\sigma_{ah}(A,\varphi) = \frac{A_a A_h \cos(\varphi)}{2} \tag{A3}$$

Covariance σ_{ah} between shank and trunk segmental motion was calculated through Eq. (A4) in the case of the postural response involving more than one frequency:

$$\sigma_{ah}(A,\omega,\varphi) = \frac{1}{T}\int_0^T \sum_{i=1}^{m} A_i^a \sin(\omega_i t+\varphi_i)\cdot \sum_{i=1}^{m} A_i^h \sin(\omega_i t)\cdot dt \tag{A4}$$

Eq. (A4) can also be written by using "change of variables" as presented above:

$$\sigma_{ah} = \frac{1}{n2\pi}\int_0^{n2\pi} \sum_{i=1}^{m} A_i^a \sin(\theta_i+\varphi_i)\cdot \sum_{i=1}^{m} A_i^h \sin(\theta_i)\cdot d\theta \tag{A5}$$

where $\omega_i t = \theta_i$

Let us assume the simplest case for the solution of the integral presented in Eq. (A5), which is "two sines" ($m = 2$). In this case, Eq. (A5) can be written as:

$$\sigma_{ah}(A,\omega,\varphi) = \frac{1}{n2\pi}\int_0^{n2\pi} (A_1^a \sin(\theta_1+\varphi_1) + A_2^a \sin(\theta_2+\varphi_2))\cdot(A_1^h \sin(\theta_1)+A_2^h \sin(\theta_2))\cdot d\theta \tag{A6}$$

Note that φ_1 and φ_2 are constants. Further, $\omega_1 t = \theta_1$ and $\omega_2 t = \theta_2$ where, $\theta_1 = k\theta_2$ and $k = \omega_1/\omega_2$, which is constant.

Thus, Eq. (A6) can now be written as:

$$\sigma_{ah}(A,k,\varphi) = \frac{1}{n2\pi}\int_0^{n2\pi} (A_1^a \sin(k\theta_2+\varphi_1) + A_2^a \sin(\theta_2+\varphi_2))\cdot(A_1^h \sin(k\theta_2)+A_2^h \sin(\theta_2))\cdot d\theta_2 \tag{A7}$$

where $d\theta$ is defined as $d\theta_2$. Eq. (A7) can be expanded as:

$$\begin{aligned}\sigma_{ah}(A,k,\varphi) = \frac{1}{n2\pi}\Big(&\int_0^{n2\pi} A_1^a \sin(k\theta_2+\varphi_1)\cdot A_1^h \sin(k\theta_2)\cdot d\theta_2 \\ &+ \int_0^{n2\pi} A_2^a \sin(\theta_2+\varphi_2)\cdot A_2^h \sin(\theta_2)\cdot d\theta_2 \\ &+ \int_0^{n2\pi} A_1^a \sin(k\theta_2+\varphi_1)\cdot A_2^h \sin(\theta_2)\cdot d\theta_2 \\ &+ \int_0^{n2\pi} A_2^a \sin(\theta_2+\varphi_2)\cdot A_1^h \sin(k\theta_2)\cdot d\theta_2\Big)\end{aligned} \tag{A8}$$

The solution of the second integral in Eq. (A8) has already been given in Eq. (A3), where it is independent of the ratio k. Thus, Eq. (A8) can be written as:

$$\sigma_{ah}(A,k,\varphi) = \frac{A_2^a A_2^h}{2}\cdot\cos(\varphi_2) + \frac{1}{n2\pi}\Big(\int_0^{n2\pi} A_1^a \sin(k\theta_2+\varphi_1) \cdot A_1^h \sin(k\theta_2)\cdot d\theta_2 + \int_0^{n2\pi} A_1^a \sin(k\theta_2+\varphi_1) \cdot A_2^h \sin(\theta_2)\cdot d\theta_2 + \int_0^{n2\pi} A_2^a \sin(\theta_2+\varphi_2) \cdot A_1^h \sin(k\theta_2)\cdot d\theta_2\Big) \quad \text{(A9)}$$

The solution of the first integral in Eq. (A9) depends on the value of k; such that:

$$\sigma_{ah}(A,k,\varphi) = \frac{A_2^a A_2^h}{2}\cdot\cos(\varphi_2) + \frac{A_1^a A_1^h}{2}\cdot\cos(\varphi_1) - \frac{A_1^a A_1^h}{kn8\pi}[\cos(\varphi_1)\sin(kn4\pi) + \sin(\varphi_1)\cdot(\cos(kn4\pi)-1)] + \frac{1}{n2\pi}\Big(\int_0^{n2\pi} A_1^a \sin(k\theta_2+\varphi_1)\cdot A_2^h \sin(\theta_2)\cdot d\theta_2 + \int_0^{n2\pi} A_2^a \sin(\theta_2+\varphi_2)\cdot A_1^h \sin(k\theta_2)\cdot d\theta_2\Big) \quad \text{(A10)}$$

"n" is an integer, being the number of cycles of perturbation, which depends on the experimental protocol. However, "k" is an intrinsic characteristic of the subject's response and if it is an integer then Eq. (A10) comes out to be:

$$\sigma_{ah}(A,k,\varphi) = \frac{A_2^a A_2^h}{2}\cdot\cos(\varphi_2) + \frac{A_1^a A_1^h}{2}\cdot\cos(\varphi_1) + \frac{1}{n2\pi}\Big(\int_0^{n2\pi} A_1^a \sin(k\theta_2+\varphi_1)\cdot A_2^h \sin(\theta_2)\cdot d\theta_2 + \int_0^{n2\pi} A_2^a \sin(\theta_2+\varphi_2)\cdot A_1^h \sin(k\theta_2)\cdot d\theta_2\Big) \quad \text{(A11)}$$

Eq. (A11) suggests that if the subject's response involves a harmonic; i.e., an integer multiple of the fundamental frequency then the solution of the first integral in Eq. (A9) becomes independent of the ratio of the two frequencies (k).

Further, if we proceed with the solution of the other two integrals in Eqs. (A10) and (A11) then the general solution for $\sigma_{ah}(A,k,\varphi)$ can be written as [36]:

$$\sigma_{ah}(A,k,\varphi) = \frac{A_2^a A_2^h}{2}\cdot\cos(\varphi_2) + \frac{A_1^a A_1^h}{2}\cdot\cos(\varphi_1) - \frac{A_1^a A_1^h}{kn8\pi}[\cos(\varphi_1)\sin(kn4\pi) + \sin(\varphi_1)\cdot(\cos(kn4\pi)-1)] + \frac{A_1^a A_2^h}{n2\pi}\Big\{\cos(\varphi_1)\cdot\Big[\frac{\sin((1-k)n2\pi)}{2(1-k)} - \frac{\sin((1+k)n2\pi)}{2(1+k)}\Big] - \sin(\varphi_1)\cdot\Big[\Big(\frac{\cos((1-k)n2\pi}{2(1-k)} + \frac{\cos((1+k)n2\pi}{2(1+k)}\Big) - \Big(\frac{1}{2(1-k)} + \frac{1}{2(1+k)}\Big)\Big]\Big\} + \frac{A_2^a A_1^h}{n2\pi} \times \Big\{\cos(\varphi_2)\cdot\Big[\frac{\sin((1-k)n2\pi)}{2(1-k)} - \frac{\sin((1+k)n2\pi)}{2(1+k)}\Big] - \sin(\varphi_2)\cdot\Big[\Big(\frac{\cos((k-1)n2\pi}{2(k-1)} + \frac{\cos((k+1)n2\pi}{2(k+1)}\Big) - \Big(\frac{1}{2(k-1)} + \frac{1}{2(k+1)}\Big)\Big]\Big\} \quad \text{(A12)}$$

where $k \neq 1$. If k is a positive integer and not equal to one; i.e., the subject's response involves an harmonic then σ_{ah} becomes independent of k and $\sigma_{ah}(A,\varphi)$ becomes

$$\sigma_{ah}(A,k,\varphi) = \frac{A_2^a A_2^h}{2}\cdot\cos(\varphi_2) + \frac{A_1^a A_1^h}{2}\cdot\cos(\varphi_1) \quad \text{(A13)}$$

References

[1] A.D. Kuo, R.A. Speers, R.J. Peterka, F.B. Horak, Effect of altered sensory conditions on multivariate descriptors of human postural sway, Exp. Brain Res. 122 (1998) 185–195.
[2] A.D. Kuo, An optimal state estimation model of sensory integration in human postural balance, J. Neural Eng. 2 (2005) S235–S249.
[3] J.P. Carroll, W. Freedman, Nonstationary properties of postural sway, J. Biomech. 26 (1993) 409–416.
[4] J.J. Collins, C.J. De Luca, Open-loop and closed-loop control of posture: a random-walk analysis of center-of-pressure trajectories, Exp. Brain Res. 95 (1993) 308–318.
[5] T. Schumann, M.S. Redfern, J.M. Furman, A. El-Jaroudi, L.F. Chaparro, Time–frequency analysis of postural sway, J. Biomech. 28 (1995) 603–607.
[6] P.J. Loughlin, M.S. Redfern, J.M. Furman, Time-varying characteristics of visually induced postural sway, IEEE Trans. Rehabil. Eng. 4 (1996) 416–424.
[7] R. Creath, T. Kiemel, F. Horak, R. Peterka, J. Jeka, A unified view of quiet and perturbed stance: simultaneous co-existing excitable modes, Neurosci. Lett. 377 (2005) 75–80.
[8] K. Guelton, S. Delprat, T.M. Guerra, An alternative to inverse dynamics joint torques estimation in human stance based on a Takagi-Sugeno unknown inputs observer in the descriptor form, Control Eng. Pract. 16 (12) (2008) 1414–1426.
[9] S. Gurses, Y. Dhaher, T.C. Hain, E.A. Keshner, Perturbation parameters associated with nonlinear responses of the head at small amplitudes, Chaos 15 (2005) 23905.
[10] F.B. Horak, L.M. Nashner, Central programming of postural movements: adaptation to altered support-surface configurations, J. Neurophysiol. 55 (1986) 1369–1381.
[11] J.S. Bendat, A.G. Piersol, Engineering Applications of Correlation and Spectral Analysis, 2nd ed., John Wiley and Sons Inc., New York, 1993.
[12] E.A. Keshner, R.V. Kenyon, J. Langston, Postural responses exhibit multisensory dependencies with discordant visual and support surface motion, J. Vestib. Res.-Equilib. Orient. 14 (4) (2004) 307–319.
[13] P.J. Loughlin, M.S. Redfern, Spectral characteristics of visually induced postural sway in healthy elderly and healthy young subjects, IEEE Trans. Neural Syst. Rehabil. Eng. 9 (2001) 24–30.
[14] K.S. Oie, T. Kiemel, J.J. Jeka, Multisensory fusion: simultaneous re-weighting of vision and touch for the control of human posture, Cogn. Brain Res. 14 (2002) 164–176.
[15] M.A. Riley, S. Clark, Recurrence analysis of human postural sway during the sensory organization test, Neurosci. Lett. 342 (2003) 45–48.
[16] E.A. Keshner, R.L. Cromwell, B.W. Peterson, Mechanisms controlling human head stabilization. II. Head–neck characteristics during random rotations in the vertical plane, J. Neurophysiol. 73 (1995) 2302–2312.
[17] J.K. Rankin, M.H. Woollacott, A. Shumway-Cook, L.A. Brown, Cognitive influence on postural stability: a neuromuscular analysis in young and older adults, J. Gerontol. A: Biol. Sci. Med. Sci. 55 (2000) M112–M119.
[18] E.A. Keshner, Head–trunk coordination during linear anterior–posterior translations, J. Neurophysiol. 89 (2003) 1891–1901.
[19] E. Jonsson, A. Seiger, H. Hirschfeld, Postural steadiness and weight distribution during tandem stance in healthy young and elderly adults, Clin. Biomech. (Bristol, Avon) 20 (2005) 202–208.
[20] R.A. Speers, A.D. Kuo, F.B. Horak, Contributions of altered sensation and feedback responses to changes in coordination of postural control due to aging, Gait Posture 16 (2002) 20–30.
[21] F.B. Horak, Mechanistic physiological aspects "Postural orientation and equilibrium: what do we need to know about neural control of balance to prevent falls?", Age Ageing 35-S2 (2006) ii7–ii11.
[22] G.L. Baker, J.P. Gollub, Chaotic Dynamics, 1st ed., Cambridge University Press, Cambridge, 1990.
[23] L.M. Nashner, Adaptation of human movement to altered environments, Trends Neurosci. 5 (1982) 358–361.
[24] A. Shumway-Cook, M. Woolacott, Attentional demands and postural control: the effect of sensory context, J. Gerontol. 55A (1999) M10–16.
[25] M.S. Redfern, R.J. Jennings, C. Martin, J.M. Furman, Attention influences sensory integration for postural control in older adults, Gait Posture 14 (2001) 211–216.
[26] J.J. Buchanan, F.B. Horak, Voluntary control of postural equilibrium patterns, Behav. Brain Res. 143 (2003) 121–140.
[27] J.J. Buchanan, F.B. Horak, Transitions in a postural task: do the recruitment and suppression of degrees of freedom stabilize posture? Exp. Brain Res. 139 (2001) 482–494.

[28] A. Bottaro, M. Casadio, P.G. Morasso, V. Sanguineti, Body sway during quiet standing: is it the residual chattering of an intermittent stabilization process? Hum. Mov. Sci. 24 (2005) 588–615.
[29] M. Woollacott, A. Shumway-Cook, Attention and the control of posture and gait: a review of an emerging area of research, Gait Posture 16 (2002) 1–14.
[30] E.A. Keshner, R.V. Kenyon, The influence of an immersive virtual environment on the segmental organization of postural stabilizing responses, J. Vestib. Res.-Equilib. Orient. 10 (4–5) (2000) 207–219.
[31] E.A. Keshner, R.V. Kenyon, Using immersive technology for postural research and rehabilitation, Assist. Technol. 16 (2004) 54–62.
[32] E. Jonsson, A. Seiger, H. Hirschfeld, One-leg stance in healthy young and elderly adults: a measure of postural steadiness? Clin. Biomech. (Bristol, Avon) 19 (2004) 688–694.
[33] F. Barbier, P. Allard, K. Guelton, B. Colobert, A.P. Godillon-Maquinghen, Estimation of the 3D center of mass excursion from force plate data during standing, IEEE Trans. Neural Syst. Rehabil. Eng. 11 (1) (2003) 31–37.
[34] B. Colobert, B. Crétual, P. Allard, P. Delamarche, Force-plate based computation of ankle and hip strategies from double-inverted pendulum model, Clin. Biomech. 21 (4) (2006) 427–434.
[35] A.L. Betker, Z.M.K. Moussavi, T. Szturm, Center of mass approximation and prediction as a function of body acceleration, IEEE Trans. Biomed. Eng. 53 (4) (2006) 686–693.
[36] S.M. Selby (Ed.), Standard Mathematical Tables, 16th ed., The Chemical Rubber Co., Cleveland, OH, 1968, pp. 409–410.